NUMERICAL SIMULATION OF SOIL LIQUEFACTION DURING THE 20 MAY 2012 M6.1 EMILIA EARTHQUAKE IN NORTHERN ITALY: THE CASE STUDY OF PIEVE DI CENTO

Anna CHIARADONNA[1], Ali G. ÖZCEBE[2], Francesca BOZZONI[3], Antonino FAMA[4], Elisa ZUCCOLO[5], Carlo G. LAI[6], Alessandro FLORA[7], Renato M. COSENTINI[8], Anna d'ONOFRIO[9], Emilio BILOTTA[10], Francesco SILVESTRI[11]

ABSTRACT

On May 20, 2012, a seismic event of moment magnitude M_W = 6.1 hit and caused severe damage on a large area in the river Po Valley, located in the northern Italy. This earthquake was characterized by extensive occurrence of soil liquefaction and basin effects lying over deep deposits. Within the scope of the European research project titled LIQUEFACT, a reference site located in the countryside near the hamlet of Pieve di Cento (at the boundary of the province of Bologna towards Ferrara) was selected as a trial field in order to assess the effectiveness of several mitigation measures against liquefaction. As a first step of the task, this paper presents the geotechnical model of the site based on in-situ investigations and pre-existing geological studies, which allowed to locate the bedrock depth. As a second step, representative input motions for the LIQUEFACT project were selected aiming at simulating the 20.V.2012 seismic event as well as three possible future scenarios with an increasing level of seismic intensity. Finally, preliminary dynamic analyses are presented, that reproduce the observed liquefaction triggering after the 2012 main event and predict the seismic soil response at the test site.

Keywords: Liquefaction analyses; numerical modeling; 2012 Emilia earthquake; LIQUEFACT

1. INTRODUCTION

On May 20, 2012 an earthquake of local magnitude M_w = 6.1 struck northern Italy, causing severe damage on a large area of the river Po Valley, in the Emilia-Romagna region (Figure 1). From the scientific point of view, the seismic event represented an important case study due to the location of the damaged sites in a deep basin structure as well as to the extensive occurrence of soil liquefaction.
The affected area is located in the south of the Po Valley, in the foreland basin of two mountain chains constituted by the Alps and the northern Appennine. A complex tectonic structure is buried under a thick layer of sedimentary fills, so that the thrusts are generally buried (Fioravante et al., 2013; Minarelli et al., 2016), with the main one being a buried ridge, known as Ferrara folds, which reaches its maximum height, about 120 m below the ground surface, near the city of Ferrara.
The subsoil is characterized by alluvial deposits of different depositional environment, which consists

[1]Post-Doc Research Associate, University of Napoli Federico II, Napoli, Italy, anna.chiaradonna@unina.it
[2]Joint Post-Doc Research Associate, University of Pavia and Politecnico di Milano, Italy, ali.ozcebe@eucentre.it
[3]Researcher, EUCENTRE, Pavia, Italy, francesca.bozzoni@eucentre.it
[4]Research Assistant, University of Pavia, Pavia, Italy, antonino.fama@eucentre.it
[5]Post-Doc Research Associate, University of Pavia, Pavia, Italy, elisa.zuccolo@eucentre.it
[6]Professor, University of Pavia, Italy, carlo.lai@unipv.it
[7]Associate Professor, University of Napoli Federico II, Napoli, Italy, flora@unina.it
[8]Post-Doc Research Associate, University of Pavia, Italy renatomaria.cosentini@unipv.it
[9]Associate Professor, University of Napoli Federico II, Napoli, Italy, donofrio@unina.it
[10]Associate Professor, University of Napoli Federico II, Napoli, Italy, bilotta@unina.it
[11]Professor, University of Napoli Federico II, Napoli, Italy, francesco.silvestri@unina.it

of alternated layers of silty-clayey deposits and sandy soils mainly constituting ancient rivers banks.
Most of the liquefaction evidences involved old river bed deposits and ancient levees of the Reno River, principally at the two villages of San Carlo (Municipality of Sant'Agostino) and Mirabello.
Liquefaction phenomena are not uncommon in this region. As pointed out by Lai et al. (2015), the database of historical liquefaction in Italy compiled by Galli (2000) includes liquefaction phenomena occurred in the Ferrara area during the 17 November 1570 M5.5 earthquake.
The LIQUEFACT project (http://www.liquefact.eu/), funded by the European Union within the Horizon 2020 framework, addresses the mitigation of risks to Earthquake Induced Liquefaction Disasters (EILD) events in European communities with a holistic approach. The project deals not only with the resistance of structures to EILD events, but also with the resilience of the collective urban community in relation to their quick recovery from an occurrence. The LIQUEACT project sets out to achieve a more comprehensive understanding of EILDs, the applications of suitable and innovative mitigation techniques, and the development of more appropriate techniques tailored to each specific scenario, for both European and worldwide situations.
Within the LIQUEFACT project, a test-site was selected jointly with local authorities (i.e. Emilia-Romagna Region and Municipality of Pieve di Cento) in order to assess the effectiveness of several mitigation measurements against liquefaction. This site, located in the Pieve di Cento (Bologna) municipality at the boundary with the Sant'Agostino (Ferrara) municipality (Figure 1), experienced widespread liquefaction manifestations after the mainshock of the 2012 seismic sequence.

Figure 1. Fault projection and epicenter of the 20.V.2012 seismic event

An extensive in-situ and laboratory investigation is currently in progress, aiming to define the dynamic behaviour of the soils before and after mitigation measures. Since liquefaction phenomenon is a local effect that typically involves the shallowest soil strata, field investigation does not exceed 15 m from the ground surface. On the other hand, the significant depth of the roof of the seismic bedrock implies the definition of a deep soil model for seismic response analysis of the site. The latter has been defined by combining previous in-situ investigations and the results of geological studies.
With a view to numerical simulations of the site, which include advanced constitutive models and detailed geometrical schemes of possible mitigation measures, the analysis domain has been restricted to the shallowest portion of the vertical soil column, consisting of a 15 m thick soil column. The limited size of the analysis domain has been required a specific definition of the input motion. Two different approaches have been considered in order to back-figure the effects of the 20.V.2012 seismic event (deterministic approach) and to reproduce the seismic demand of the site for three different return periods (probabilistic approach).
Finally, preliminary dynamic analyses in effective stresses have been carried out on the shallow profile to assess the reliability of the assumed hypotheses and to predict the seismic soil response of the site

2. GEOTECHNICAL MODEL

The soil deposits at the testing site in Pieve di Cento have been characterized on the basis of the first outcomes from the campaign carried out in LIQUEFACT project, whose results were integrated with geological and geotechnical data retrieved from the literature and from previous investigation campaigns acquired from the technical staff of the Emilia-Romagna Region. Ground conditions near of the test site is gathered from the study of Minarelli et al. (2016) presenting the geological information (Martelli and Romani, 2013; Paolucci et al., 2015) supported by also deep downhole (DH) investigations along a ~35 km-long segment in the Po Plain, starting from Cento and ending in Occhiobello (Figure 2a). The closest distances from the test site to the investigation line and nearest deep downhole investigation are in the order of 2 and 5 kilometers, respectively.
Figure 2b shows geological section provided by Minarelli et al. (2016), which is a modified version of Martelli and Romani (2013), Paolucci et al. (2015). More detailed information on the depth of geological interfaces was obtained from a geological section from CARG Project (http://www.isprambiente.gov.it), which includes two deep boreholes, called as Pievedicento001 (down to 1.5 km) and S13 CARG (down to 70 m) in Figure 2a, respectively. Geological section provided by Minarelli et al. (2016) is presented in Figure 2b, which is a modified version of Paolucci et al. (2015). Minarelli et al. (2016) noted that the depth of the seismic bedrock (V_S=800 m/s) is not clearly determined, thus in the current work the bedrock level is taken at the top of Marine Quaternary formation (QM), located 230 m below the ground level.

(a)

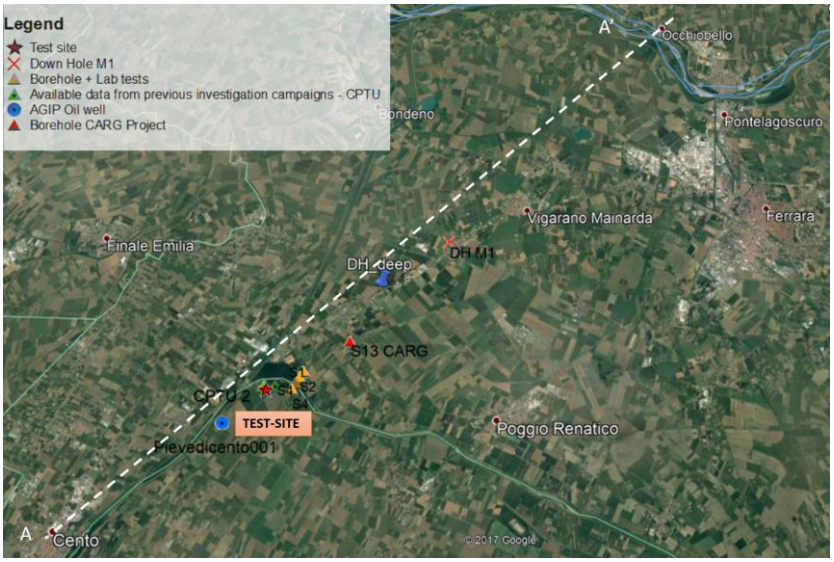

(b)

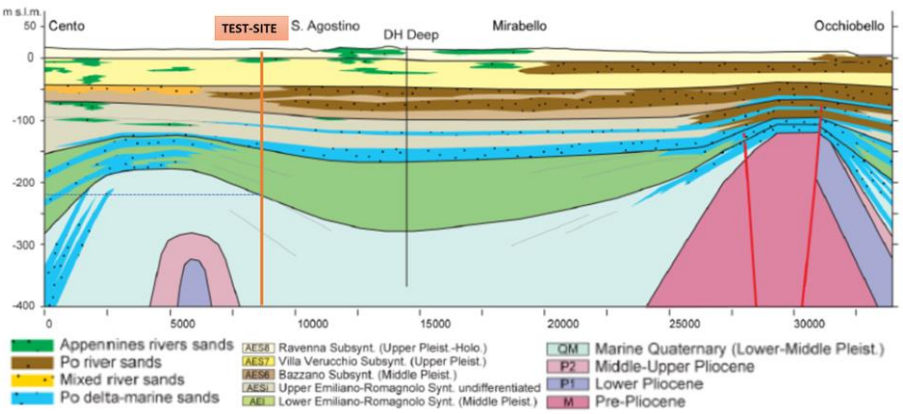

Figure 2. (a) In-situ investigation and geological section across the test-site. (b) Geological A-A' section of Po Valley (after Paolucci et al., 2015; after Minarelli et al., 2016). Interface of QM (Marine Quaternary) is used as the discontinuity for the seismic bedrock. Orange line shows the location of the test site

Because of the large depth of the bedrock, a deep soil profile was defined by using the information provided by Minarelli et al. (2016) on the spatial distributions of the layers and on the ranges of shear wave velocity V_S associated with different geological units. On the other hand, specific site investigation in the shallowest soil layers allowed to characterize the soil profile in the uppermost 15 m below the ground level.

The soil column consists of a sequence of silty-clay and sandy soil deposits, divided into several geological units, called subsystems (Minarelli et al., 2016). Shear wave velocity and thickness were assigned to every subsystem based on the DH presented by Minarelli et al. (2016) and on retrieved geological sections. Dynamic material curves were generated by considering Darendeli (2001) framework, in which the plasticity index is selected as 0 and 30 for 0-6 and 6-220 meters, respectively (Table 1). Apart from the main influencing parameters (mean effective confining stress and plasticity index), the other required parameters were assumed as: over-consolidation ratio OCR=1, excitation frequency 1 Hz and number of cycles N=10. Figure 3a shows the soil layering and the related V_S profile obtained by interpreting all the available information.

Figure 3b focuses on the shallow layering and the shear wave velocity profile as identified from a borehole and a Cross-Hole test carried out at the site. The soil column consists of a sandy silt layer overlaying a silty sand layer that is supposed to be the liquefiable layer. In the considered borehole, a thin clayey layer is identified in the silty sand deposits between 4.2 and 4.8 m depth. The same formation is in the soil profile beyond 6 m depth from the ground surface, as shown by combining the data from the 10 m borehole and pre-existing Cone Penetration Tests (Figure 2a). The shear wave velocity profile was defined from the interpretation of the results of the Cross-Hole test, shown in Figure 3b. A linear trend has been identified in the clay layer; it has been adopted for the whole clay formation and the interbedded thin clay layer, which was not revealed by the Cross-Hole test.

Since site-specific laboratory tests are currently in progress, the non-linear soil properties have been modelled assuming shear modulus reduction and damping curves of the soil deposits at Scortichino (Figure 1), where resonant column tests were performed (Tonni et al., 2015). At this site, 20 km far from the test-site, sandy and clayey layers have the same geological background and a grain size distribution similar to those in Pieve di Cento.

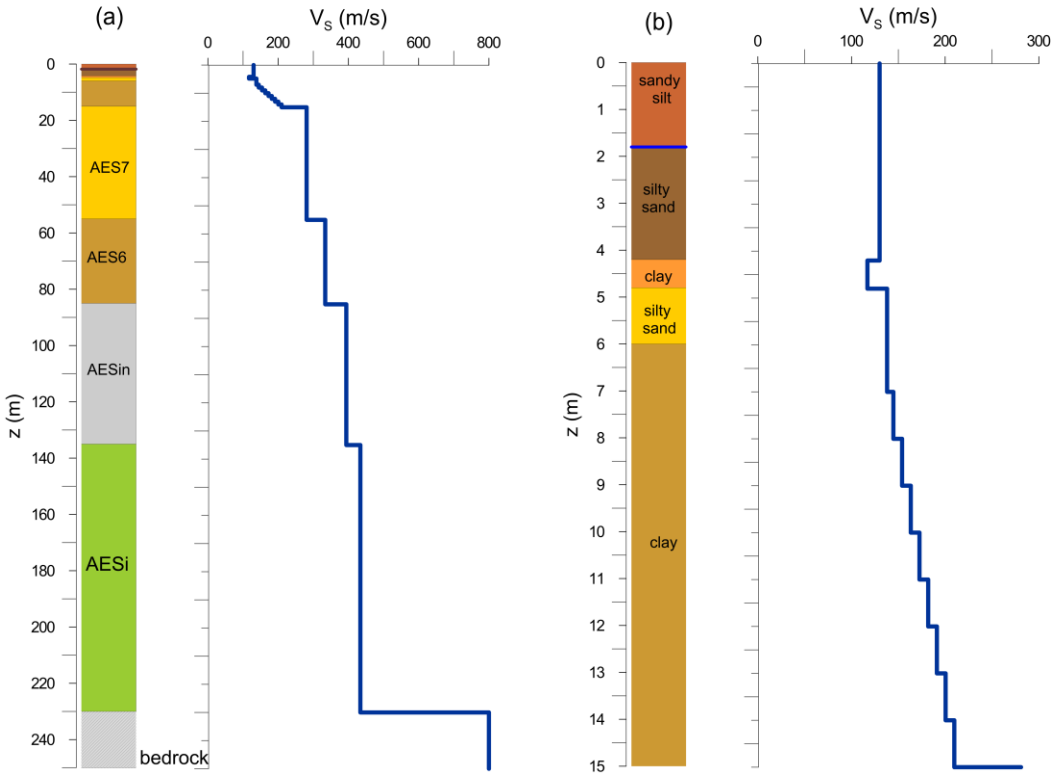

Figure 3. Shear wave velocity profile used for Pieve di Cento site. (a): in larger depth range, (b): in smaller depth range

Table 1. Geotechnical model for Pieve di Cento site

Profile	Soil	H (m)	γ (kN/m^3)	V_s (m/s)	G/G_0 (γ) and D (γ) curves
Shallow	Sandy silt	1.8	16	130	Scortichino sand (Chiaradonna et al., 2018a)
	Silty sand	2.4	18.9	130	Scortichino sand (Chiaradonna et al., 2018a)
	Clay	0.6	18.9	117	Scortichino clay (Chiaradonna et al., 2018a)
	Silty sand	1.2	18.9	138	Scortichino sand (Chiaradonna et al., 2018a)
	Clay	9	18.9	138 ÷ 210	Scortichino clay (Chiaradonna et al., 2018a)
Deep	AES7	10	19.62	281	Darendeli curves (σ'_{m0}=1.25 atm, PI=30)
	AES7	10	19.62	281	Darendeli curves (σ'_{m0}=2.00 atm, PI=30)
	AES7	10	19.62	281	Darendeli curves (σ'_{m0}=2.50 atm, PI=30)
	AES7	10	19.62	281	Darendeli curves (σ'_{m0}=3.25 atm, PI=30)
	AES6	15	19.62	344	Darendeli curves (σ'_{m0}=4.00 atm, PI=30)
	AES6	15	19.62	344	Darendeli curves (σ'_{m0}=5.00 atm, PI=30)
	AESin	50	19.62	394	Darendeli curves (σ'_{m0}=7.00 atm, PI=30)
	AESi	95	19.62	434	Darendeli curves (σ'_{m0}=7.00 atm, PI=30)
	Halfspace	-	22	800	D_0 = 0.5 %

3. INPUT MOTION

In this Section, two different approaches are presented to define the ground motion at the depth of 15 meters for analyzing the dynamic response of the shallow soil profile identified in Section 2.
The former approach (presented in Section 3.1) aims to back-figure the 20.V.2012 seismic event, whereas the latter (presented in Section 3.2) was adopted in order to reproduce the expected seismic demand of the site within a probabilistic framework, for three different return periods: 475, 975 and 2475 years.

3.1 Deterministic approach (Approach 1)

The first approach aims to reproduce the seismic demand induced at the reference test site by the mainshock of the 2012 Emilia seismic sequence, using the recorded acceleration time histories.
The mainshock of the Emilia 2012 earthquake sequence occurred on May 20, 2012 at 02:03:53 UTC time. The MRN station of the Italian strong-motion network (RAN), located in Mirandola town, is the closest to the epicenter (Figure 1) and recorded a peak ground acceleration, PGA, as high as 0.273g (Chiaradonna et al., 2018a).
This record cannot be used directly as a reference input motion in a seismic site response analysis, because the station is located on a deep layer of soft ground, with an equivalent shear wave velocity $V_{S,30}$ = 208 m/s, i.e. a Class C site according to Eurocode 8 (EC8). As previously mentioned, the 2012

seismic sequence affected an alluvial plain with a significant depth of the seismic bedrock, hence the closest stations located on a rock outcrop lie too far from the epicenter. To overcome this problem, Chiaradonna et al. (2018a) deconvolved the EW component of the acceleration record at MRN station to the bedrock; thereafter, the deconvolved outcrop motion was scaled down to account for the epicentral distance of the test site, according to the attenuation law proposed by Bindi et al. (2011).
In the end, the deconvolved motion was propagated from the assumed bedrock (230 m deep) up to 15 m depth (Figure 3a). The obtained ground motion at 15 m is shown in Figure 4 in terms of acceleration time history (Figure 4a) with the correspondent acceleration response spectrum (Figure 4b).

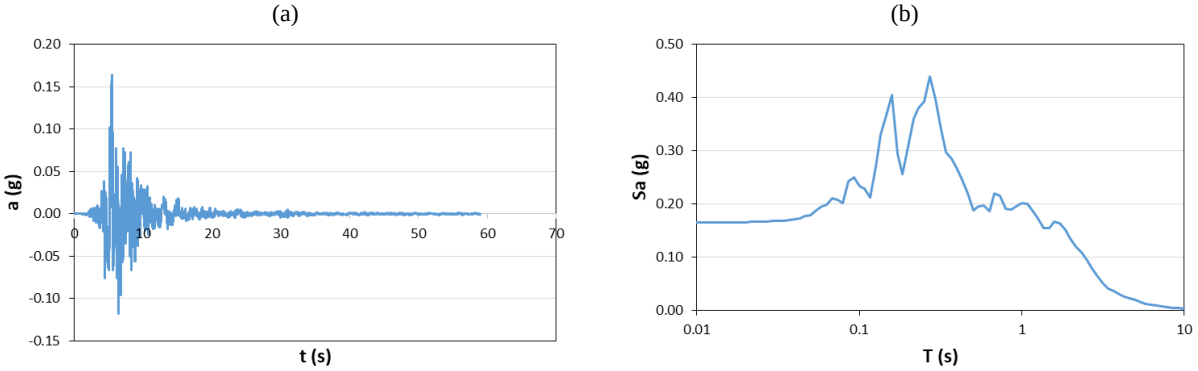

Figure 4. Deconvolved input motion at 15 m (a): acceleration time history, (b): acceleration response spectrum

3.2 Probabilistic approach (Approach 2)

In the second approach, the definition of the input motion is carried out in two steps: (1) selecting a number of rock outcrop ground motions and scaling them according to PEER methodology (PEER 2010a, b) to obtain spectral compatibility and (2) propagate the rock motions from the seismic bedrock location (230 m deep) up to 15 m. Details of the steps (1) and (2) are presented in Section 3.2.1 and 3.2.2, respectively.

3.2.1 Selection of the natural rock outcrop motions

As a first step, a set of 7 natural accelerograms recorded on outcropping rock was selected for each considered return period (i.e. 475, 975, and 2475 years). The selection was made using an updated version of the program ASCONA (Corigliano et al., 2012), which provides a set of recordings satisfying several criteria (such as magnitude, distance, spectral shape), with the additional requirement of compatibility with a target spectrum (in this case, the elastic acceleration response spectrum prescribed by the Italian design code for each considered hazard level), in a specified range of periods (in this case, 0.01 s to 0.1 s). Records are taken from an internal database composed by accelerograms collected from accredited strong motion databases (ESM - Engineering Strong-Motion database version 0.1, PEER NGA-West2 and KiK-net strong motion database). In order to ensure compatibility with the target spectrum, recordings are scaled following the PEER scaling approach, given in Equation (1):

$$SF = \frac{\sum_i w(T_i)\ln\left(S_{a,tar}(T_i)/S_{a,rec}(T_i)\right)}{\sum_i w(T_i)} \quad (1)$$

where SF is the scaling factor, w is a *weight function* defined for 261 spectral periods T_i evenly-spaced in log scale from 0.01s to 4 sec, $S_{a,rec}$ (T_i) is the elastic acceleration spectral ordinate of the recorded spectrum at T_i, $S_{a,tar}(T_i)$ is the elastic acceleration spectral ordinate of the target spectrum at T_i, and $w_i(T_i)$ is the weighting factor for T_i. In this work, $w_i = 0.5$ is used for T= [0, 0.1[s, $w_i = 1.0$ is used for T= [0.1, 1.0] s, and $w_i = 0.1$ is used for T_i=]1.0, 4.0] s. Among the sets of accelerograms satisfying the user-defined criteria and the spectrum-compatibility requirement, the set selected by ASCONA, is characterized by the minimum average misfit between the mean response spectrum of the recordings and the target spectrum. The 21 selected accelerograms are listed in Table 2.

Table 2. Details regarding selected and scaled sets of 7 natural, rock outcrop acceleration motions for return periods of 475, 975, and 2475 years. T_r: return period in years, M_w: moment magnitude, R_{ep}: epicentral distance, *SF*: scale factor calculated from Eq. (1), *Source File*: filename in the parent database

GM_ID	T_r *(years)*	M_w	R_{ep} *(km)*	*SF*	*Source File*
GM11	475	5.74	12.57	1.51	NGA RSN146_COYOTELK_G01320.AT2
GM12	475	5.90	10.10	1.79	ESM IT.ATN..HNN.D.19840507.174943.C.ACC.ASC
GM13	475	6.69	38.07	0.91	NGA RSN1091_NORTHR_VAS000.AT2
GM14	475	6.60	26.00	1.21	KiKnet 0KYH070010061330.NS2
GM15	475	6.60	62.00	1.24	KiKnet SAGH050503201053.EW2
GM16	475	5.20	11.80	2.26	ESM IT.AQP..HNN.D.20090409.005259.C.ACC.ASC
GM17	475	6.10	97.00	1.65	KiKnet MYGH041103280724.EW2
GM21	975	6.90	62.90	0.95	ESM EU.HRZ..HNE.D.19790415.061941.C.ACC.ASC
GM22	975	5.74	12.57	2.02	NGA RSN146_COYOTELK_G01320.AT2
GM23	975	5.90	10.10	2.39	ESM IT.ATN..HNN.D.19840507.174943.C.ACC.ASC
GM24	975	6.93	28.64	0.56	NGA RSN765_LOMAP_G01000.AT2
GM25	975	6.69	38.07	1.19	NGA RSN1091_NORTHR_VAS090.AT2
GM26	975	6.60	31.00	0.89	KiKnet SMNH100010061330.EW2
GM27	975	6.60	37.00	2.21	KiKnet SAGH010503201053.NS2
GM31	2475	6.90	62.90	1.33	ESM EU.HRZ..HNE.D.19790415.061941.C.ACC.ASC
GM32	2475	5.74	12.57	2.82	NGA RSN146_COYOTELK_G01320.AT2
GM33	2475	5.90	10.10	3.34	ESM IT.ATN..HNN.D.19840507.174943.C.ACC.ASC
GM34	2475	6.93	28.64	0.59	NGA RSN765_LOMAP_G01000.AT2
GM35	2475	6.69	38.07	1.66	NGA RSN1091_NORTHR_VAS090.AT2
GM36	2475	6.60	31.00	1.24	KiKnet SMNH100010061330.EW2
GM37	2475	6.60	37.00	3.09	KiKnet SAGH010503201053.NS2

3.2.2 Propagation of the scaled rock motions up to the depth of 15 meters

Under ideal conditions, the use of a well-calibrated nonlinear constitutive model working in effective stresses would be sufficient accurate to model the dynamic response of the soil profile. However, this approach requires an extended set of in-situ and laboratory tests on the geotechnical layers, not available yet at the stage of input motion definition under the scope of LIQUEFACT. Therefore, instead of carrying out a detailed effective-stress based analysis to define the ground motion through the whole profile, attention has been given to the uppermost 15 meters, for which more information were available, using the following models, listed in order of increasing complexity:

i. classical equivalent-linear model;
ii. nonlinear hysteretic model implemented in FLAC (Itasca, 2016) with Masing-type reversals;
iii. loosely-coupled effective stress based model for the top 0-6 meters and model (ii) for the rest. For the effective stress model the Finn-type formulation (Byrne, 1991) is assumed, with the use of Mohr-Coulomb yield surface. The definition of volumetric-shear strain coupling is provided by Equation (2):

$$\frac{\Delta\varepsilon_{vd}}{\gamma} = C_1 \exp\left(-C_2 \frac{\varepsilon_{vd}}{\gamma}\right) \tag{2}$$

where γ is the current shear strain, ε_{vd} is the cumulative irreversible volumetric strain, $\Delta\varepsilon_{vd}$ is the irreversible volumetric strain increment; C_1 and C_2 are model parameters: $C_1=7600(D_r)^{-2.5}$ for relative density (D_r = 35%) and $C_2=0.4/C_1$.

It is worth noting that for all models (i), (ii) and (iii), the shear modulus degradation relations of

Darendeli (2001) were adopted, as discussed in Section 2.1. In addition, for model (i) only, the corresponding damping ratio-shear strain relation is assigned.

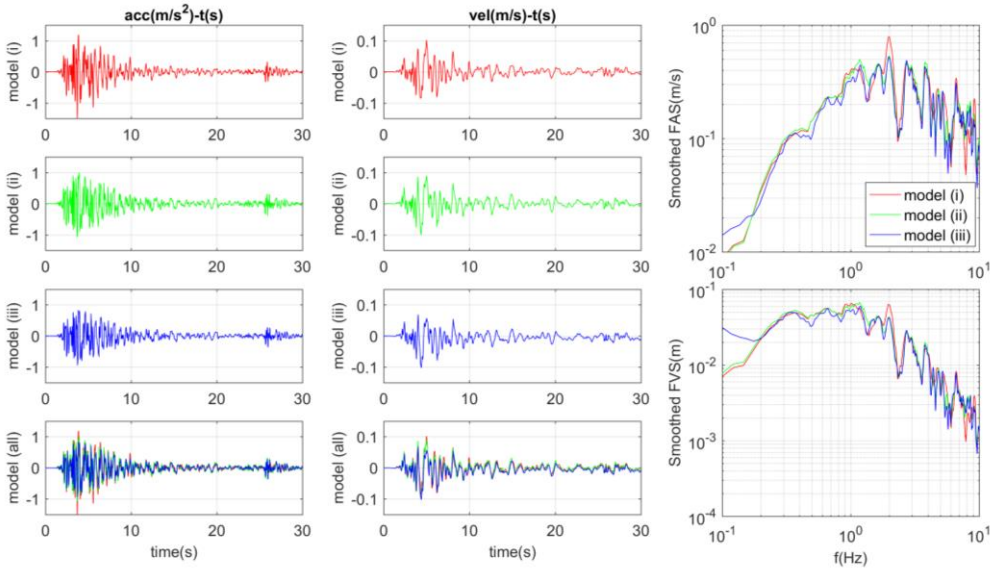

Figure 5. Comparison of acceleration and velocity responses in temporal and frequency domain at depth of 15 meters by using the illustrative case of GM23 (see Table 2)

In Figure 5, as an example a comparison of the acceleration and velocity response is shown for methods (i)-(iii) in both time and frequency domains for the illustrative input motion of GM23. The results are similar, and therefore it is expected that all the three models would result in similar liquefaction response for the shallower depths, as was demonstrated for different input motions.
For the sake of brevity, in the following section (3.3) only method (ii) is used, due to its applicability in time domain and to the lower amount of calibration parameters needed.

3.3 Comparison of Approaches 1&2

In this section, the input motions, generated through Approaches 1 and 2, are compared in terms of strong ground motion characteristics that are shown to be well correlated with the triggering of liquefaction, as: I_A, CAV_5, MHA (Kramer and Mitchell, 2006). Here, I_A is the Arias intensity, CAV_5 is the cumulative absolute velocity after the first exceedance of 0.05 m/s^2 acceleration threshold, and MHA is the Maximum Horizontal Acceleration (used as peak horizontal acceleration for outcrop conditions). In Figure 6, the abovementioned strong ground motion parameters resulting from the 20.V.2012 motion at 15 meters (represented by EV) are compared with statistical values corresponding to the motions obtained through following Approach 1 (i.e. *method b* of Section 3.2) for all of the three sets corresponding to different return periods: 475, 975, and 2475 years. EV shows a reasonable agreement with T_r=475 years for CAV_5 and I_A, whereas for MHA it is in a better agreement with T_r=975 years.

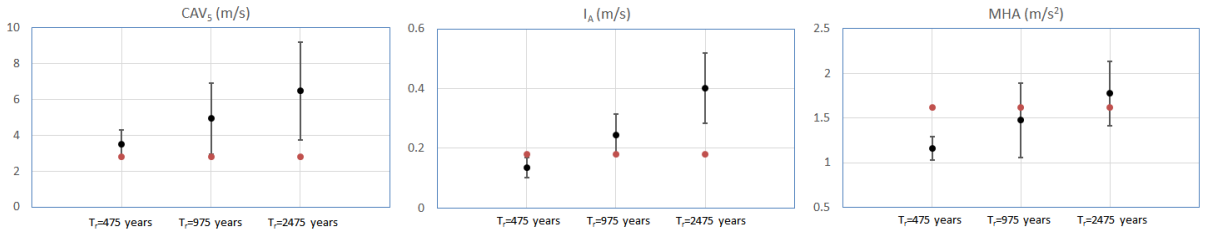

Figure 6. Comparison of liquefaction-related strong ground motion parameters for a motion at 15 m depth. Red points: 20.V.2012 event (EV), black points: mean values for three different hazard level, error bars: +/-1 standard deviation.

4. DYNAMIC NUMERICAL ANALYSES

Dynamic analyses on the shallow soil profile were carried out in effective stresses according to a loosely coupled approach. The adopted geotechnical model has been described in §2. The depth of the ground water table has been assumed at 1.8 m below the ground level as shown by the in-situ investigations and a pore-water pressure model has been assigned to the silty sand layers (Table 1 and Figure 3b).

4.1 Non-linear analysis using input motion from Approach 1

For the input signal defined through the deterministic approach (Approach 1, §3.1), simulating the mainshock of the 2012 seismic sequence, two different semi-empirical models were adopted: the loosely coupled model proposed by Byrne (1991), as described in §3.2.2 (model iii), and a simplified pore water pressure model based on accumulation of shear stress recently developed by Chiaradonna et al. (2018b).
The Byrne model, implemented in FLAC (Itasca, 2016), requires the definition of a value of relative density. In this case the value $D_r = 35\%$ has been assumed based on CPTU results interpretation.
As far as the second model is concerned, the excess pore water pressure build-up in the saturated soils has been calculated using a simplified model based on the accumulation of shear stress (Chiaradonna et al., 2018b), which is implemented in the 1D computer code SCOSSA (Tropeano et al., 2016). Figure 7 reports the results of simulations performed by the two different models in terms of maximum profile of acceleration and excess pore pressure ratio, r_u, defined as the ratio between the excess pore pressure and the initial effective vertical stress.

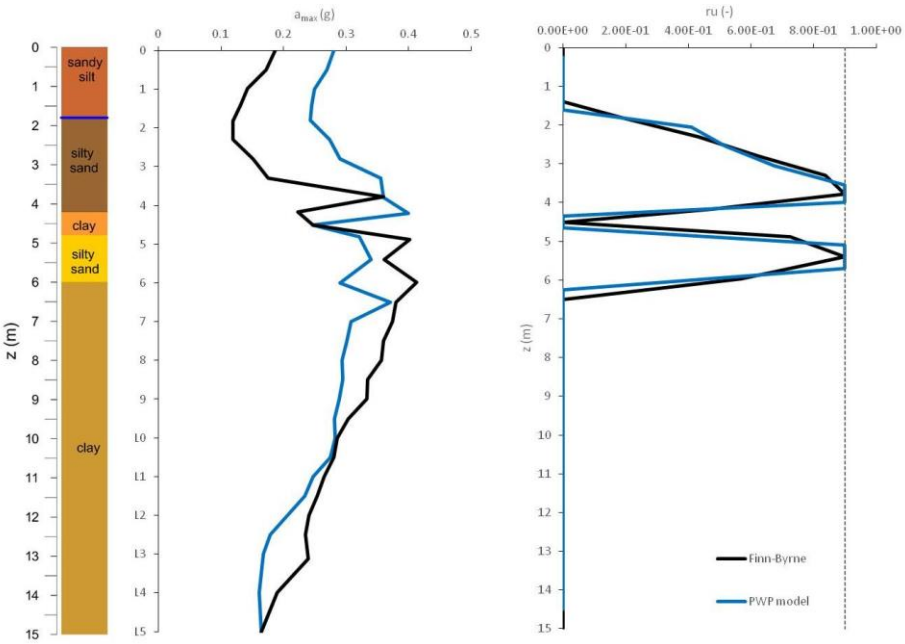

Figure 7. Effective stress analysis for the approach 1 input motion: subsoil profile; maximum acceleration and maximum pore pressure ratio

The acceleration profile is characterized by reduced values above the liquefiable silty sand soils, caused by the sharp reduction in shear wave velocity in the liquefied/degraded soil layer that works as an isolator. Excess pore water pressure ratio profiles show that both models are able to predict the occurrence of the observed liquefaction.

4.2 Non-linear analysis using input motion from Approach 2

In the framework of a probabilistic approach to define the input signals for three possible future

scenarios (Approach 2), the effective stress analyses have been carried out using SCOSSA only and applying at the base of the profile the 21 input motions selected in §3.2. Figure 8 (a,b,c) compares the results of the simulations performed for the three return periods in terms of maximum profile of acceleration and excess pore pressure ratio, r_u,. For each set of signals the mean profile was computed (black line in Figure 8). The mean acceleration exhibits at the surface a slightly increasing value from 0.23 to 0.26 g moving from 475 to 2475 years as return period, due to the increasing level of the seismic intensity. On the other hand, the excess pore pressure profiles show that the liquefaction is attained in most of the cases, even though the mean profile did not reach full liquefaction (i.e. $r_u = 0.9$) for return period of 475 years.

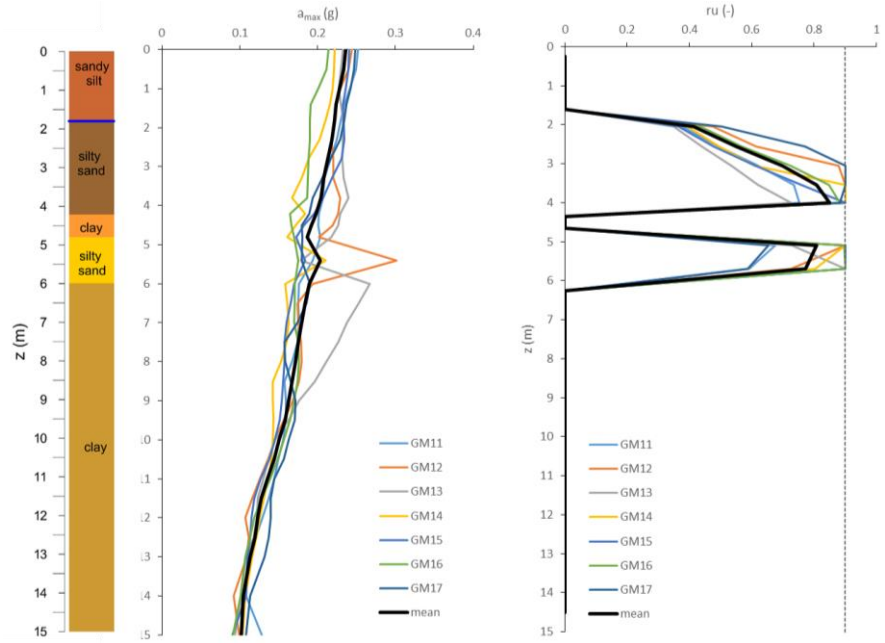

Figure 8a. Effective stress analysis for Approach 2 input motions: subsoil profile; maximum acceleration and maximum pore pressure ratio for 475 years

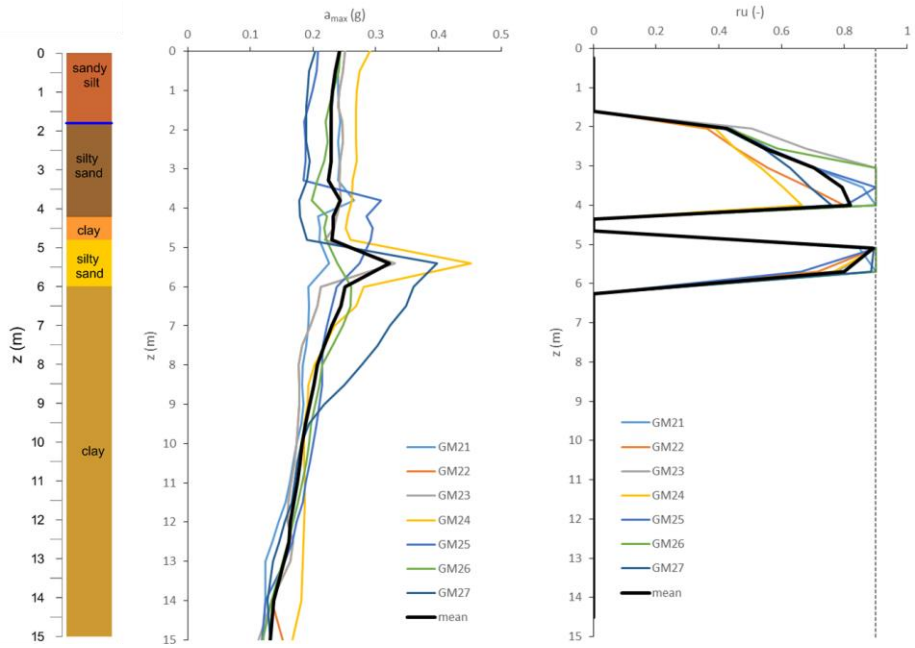

Figure 8b. Effective stress analysis for Approach 2 input motions: subsoil profile; maximum acceleration and maximum pore pressure ratio for 975 years

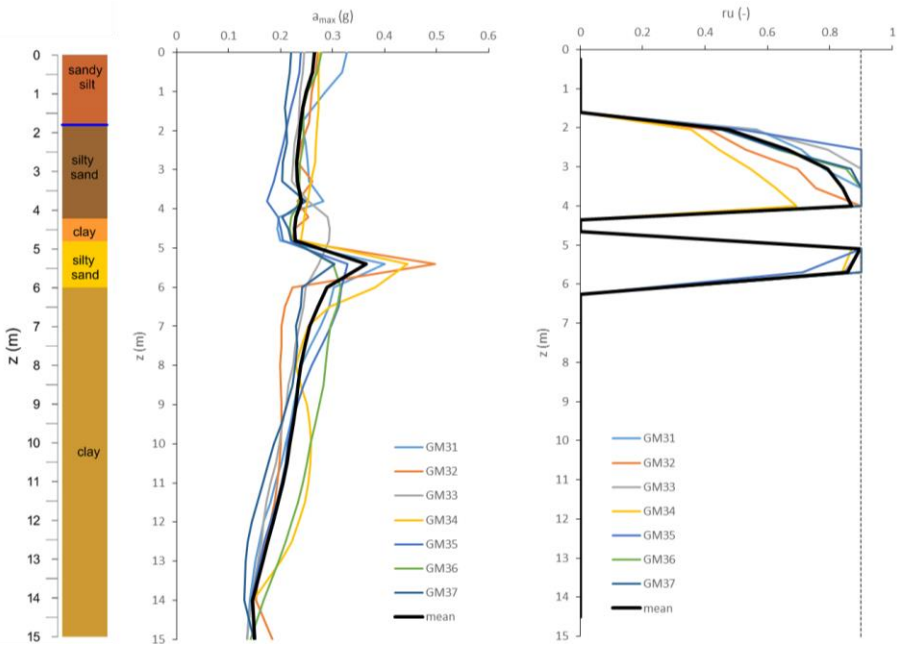

Figure 8c. Effective stress analysis for Approach 2 input motions: subsoil profile; maximum acceleration and maximum pore pressure ratio for 2475 years

5. CONCLUSIONS

In this paper, focus has been given to the two main tasks of defining the ground motion at 15 m depth and numerically investigating the observed soil liquefaction due to the event of 20.V.2012 at the selected site of Pieve di Cento, Italy.
To achieve the former task, two different approaches have been adopted: (1) a deterministic approach by directly using the deconvolution of a recorded signal for the event of 20.V.2012; (2) a probabilistic approach, based on the use as input motion of three sets of 7 real accelerograms compatible to 475-year, 975-year, and 2475-year return period elastic acceleration response spectra.
Once the input ground motion time histories were selected, two different models have been adopted to achieve the second task: (1) a loosely coupled effective stress model proposed by Byrne (1991) and (2) a simplified model using the concept of stress accumulation. It is concluded that both models were able to trigger liquefaction, as it was observed at the site during the event.
Finally, the second model (Chiaradonna et al., 2018b) was used to assess the potential of liquefaction in the site for the three possible future scenarios defined by the probabilistic approach.

6. ACKNOWLEDGMENTS

This work was carried out as part of the European project Horizon 2020 LIQUEFACT “Assessment and Mitigation of liquefaction potential across Europe: A holistic approach to protect structures infrastructures for improved resilience to earthquake-induced liquefaction disasters” (grant agreement No. 700748). We would like to express our gratitude to the administrations of Emilia-Romagna Region (in particular to Dr. Luca Martelli) and to the Municipality of Pieve di Cento (especially to Eng. Luca Borsari). A special thank also to Mr. Rino Govoni, owner of the area selected as test site.

7. REFERENCES

Bindi D, Pacor F, Luzi L, Puglia R, Massa M, Ameri G, et al. (2011). Ground motion prediction equations derived from the Italian strong motion database. *Bulletin of Earthquake Engineering*, 9(6):1899-1920.

Byrne, PM (1991). A cyclic shear-volume coupling and pore pressure model for sand. *International Conference on Recent Advances in Geotechnical Earthquake Engineering and Soil Dynamics, I*.

Chiaradonna A, Tropeano G, d'Onofrio A, Silvestri F (2018a). Interpreting the deformation phenomena of a levee damaged during the 2012 Emilia earthquake. *Special Issue Soil Dynamics and Foundation Engineering* (submitted).

Chiaradonna A, Tropeano G, d'Onofrio A, Silvestri F (2018b). Development of a simplified model for pore water pressure build-up induced by cyclic loading. *Bulletin of Earthquake Engineering* (submitted).

Corigliano M, Lai CG, Rota M, Strobbia CL (2012). ASCONA: automated selection of compatible natural accelerograms. *Earthquake Spectra*, 28(3): 965-987.

Darendeli MB (2001). Development of a new family of normalized modulus and material damping curves. PhD Thesis, The University of Texas at Austin.

Fioravante V, Giretti D, Abate G, Aversa S, Boldini D, Capilleri PP et al. (2013). Earthquake geotechnical engineering aspects of the 2012 Emilia-Romagna earthquake (Italy). *Proceedings of the 7th international conference on case histories in geotechnical engineering*, Chicago, Illinois, USA.

Galli P (2000). New empirical relationships between magnitude and distance for liquefaction, *Tectonophysics* 324, 169-187.

Itasca (2016). FLAC, Fast Lagrangian Analysis of Continua, version 8.0 Computer Program and the User's Guide, Itasca Consulting Group Inc., Thrasher Square East.

Lai CG, Bozzoni F, Mangriotis MD, Martinelli M (2015). Soil liquefaction during the May 20, 2012 M5.9 Emilia earthquake, Northern Italy: field reconnaissance and post-event assessment. *Earthquake Spectra*, 31(4), 2351-2373.

Kramer SL, Mitchell RA (2006). Ground motion intensity measures for liquefaction hazard evaluation. *Earthquake Spectra*, 22(2): 413-438.

Martelli L, Romani M (2013). Microzonazione sismica e analisi della condizione limite per l'emergenza delle aree epicentrali dei terremoti della pianura emiliana di maggio-giugno 2012 (Ordinanza del commissario delegato n. 70/2012), Relazione Illustrativa (in Italian); http://ambiente.regione.emilia-romagna.it

Minarelli L, Amoroso S, Tarabusi G, Stefani M, Pulelli G (2016). Down-hole geophysical characterization of middle-upper Quaternary sequences in the Apennine Foredeep, Mirabello, Italy. *Annals of Geophysics*, 59(5), doi: 10.4401/ag-7114.

Paolucci E, Albarello D, D'Amico S, Lunidei E, Martelli L, Mucciarelli M, Pileggi D (2015). A large scale ambient vibration survey in the area damaged by May-June 2012 seismic sequence in Emilia Romagna, Italy. *Bulletin of Earthquake Engineering*, 13(11):3187-3206.

PEER (2010a). Technical report for the PEER ground motion database web application-Beta Version-October 1, 2010.

PEER (2010b). User's Manual for the PEER ground motion database web application-Beta Version-October 1, 2010.

Tonni L. Gottardi G, Amoroso S, Bardotti R, Bonzi L, Chiaradonna A, d'Onofrio A, Fioravante V, Ghinelli A, Giretti D, Lanzo G, Madiai C, Marchi M, Martelli L, Monaco P, Porcino D, Razzano R, Rosselli S, Severi P, Silvestri F, Simeoni L, Vannucchi G, and Aversa S (2015). Interpreting the deformation phenomena triggered by the 2012 Emilia seismic sequence on the Canale Diversivo di Burana banks. *Italian Geotechnical Journal*, 2: 28 - 58 (in Italian).

Tropeano G, Chiaradonna A, d'Onofrio A, Silvestri F (2016). An innovative computer code for 1D seismic response analysis including shear strength of soils. *Géotechnique*, 66(2): 95–105.